Molecular Dynamics of Methylamine, Methanol, and Methyl Fluoride Cations in Intense 7 Micron Laser Fields

ARTICLE *in* THE JOURNAL OF PHYSICAL CHEMISTRY A · SEPTEMBER 2014

Impact Factor: 2.69 · DOI: 10.1021/jp507251e · Source: PubMed

THE JOURNAL OF PHYSICAL CHEMISTRY A

Article

pubs.acs.org/JPCA

Molecular Dynamics of Methylamine, Methanol, and Methyl Fluoride Cations in Intense 7 Micron Laser Fields

Bishnu Thapa and H. Bernhard Schlegel*

Department of Chemistry, Wayne State University, Detroit, Michigan 48202, United States

Supporting Information

ABSTRACT: Fragmentation and isomerization of methylamine ($CH_3NH_2^+$), methanol (CH_3OH^+), and methyl fluoride (CH_3F^+) cations by short, intense laser pulses have been studied by ab initio classical trajectory calculations. Born−Oppenheimer molecular dynamics (BOMD) on the ground-state potential energy surface were calculated with the CAM-B3LYP/6-31G(d,p) level of theory for the cations in a four-cycle laser pulse with a wavelengths of 7 μm and intensities of 0.88×10^{14} and 1.7×10^{14} W/cm^2. The most abundant reaction path was $CH_2X^+ + H$ (63−100%), with the second most favorable path being $HCX^+ + H_2$ (0−33%), followed by isomerization to CH_2XH^+ (0−8%). C−X cleavage after isomerization was observed only in methyl fluoride. Compared to random orientation, CH_3X^+ with the C−X aligned with the laser polarization gained energy nearly twice as much from laser fields. The percentage of $CH_3^+ + X$ dissociation increased when the C−X bond was aligned with the laser field. Alignment also increased the branching ratio for H_2 elimination in $CH_3NH_2^+$ and CH_3OH^+ and for isomerization in CH_3OH^+.

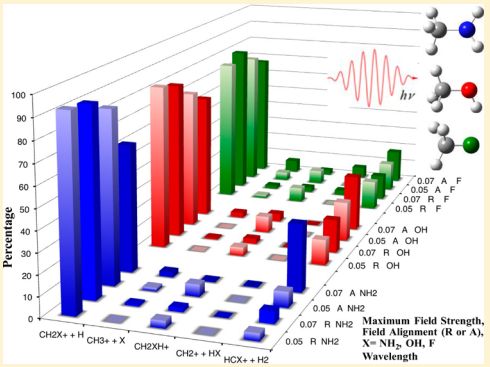

INTRODUCTION

In simulations with Born−Oppenheimer molecular dynamics, we have shown that small molecular ions can absorb substantial amounts of energy from intense mid-IR laser pulses and undergo rapid reactions before intramolecular vibrational energy redistribution occurs.[1,2] In the present work, we examine the isomerization and fragmentation of $CH_3NH_2^+$, CH_3OH^+, and CH_3F^+ by short intense 7 μm laser pulses. This work is motivated by recent studies of methanol cations by Yamanouchi and co-workers using pump−probe coincidence momentum imaging.[3−10] A 40 fs, 800 nm pump pulse produced the monocation, and a probe pulse, delayed by 100−800 fs, ionized it to the dication. Coincidence imaging of specific fragmentations of the dication, $CH_3OH^{2+} \rightarrow CH_3^+ + OH^+$ and $CH_2OH_2^{2+} \rightarrow CH_2^+ + H_2O^+$, showed that isomerization occurred during and shortly after the pulse.[9,10]

In prior work, we used ab initio classical trajectory calculations to investigate the dynamics of the methanol monocation on the ground-state potential energy surface in the presence of a strong laser field.[11,12] Classical dynamics simulations showed that ground-state methanol cation gained only a few kcal/mol from an 800 nm laser field, suggesting that excited states and coupled nuclear−electron dynamics may be important for interactions with 800 nm laser pulses. By contrast, mid-IR laser fields interacted directly with the molecular vibrations of CH_3OH^+, depositing enough energy to cause significant amounts of isomerization and dissociation on the ground-state surface.[12] Our simulations of $ClCHO^+$, CF_3Br^+, and $C_6H_5I^{2+}$ showed that intense mid-IR pulses were able to selectively enhance specific reaction channels for aligned molecules.[1,2] Therefore, in the present paper, we focus on mid-IR laser pulses and consider both randomly oriented and aligned molecules.

In the current study, we explore the effect of changes in potential energy surface on the reactions driven by the laser field. Like CH_3OH^+, the reaction channels for $CH_3NH_2^+$ and CH_3F^+ include H elimination, H_2 loss, $CH_3X \rightarrow CH_2XH$ isomerization, and C−X dissociation. Differences in the barriers for these reactions range from 10 (H elimination) to over 50 kcal/mol (C−X dissociation). Born−Oppenheimer molecular dynamics have been used to model the isomerization and fragmentation of both randomly oriented and aligned CH_3X^+ in short, intense laser pulses. As in earlier studies,[11,12] the simulations used wavelengths of 7 μm and intensities of 0.88×10^{14} and 2.9×10^{14} W/cm^2 (field strengths of 0.05 and 0.07 au).

METHODS

Electronic structure calculations were carried out with the development version of the Gaussian series of programs.[13] Field-free reaction energetics were calculated at the CAM-B3LYP/6-31G(d,p) and CBS-QB3 levels of theory.[14,15] Molecular dynamics simulations in intense laser fields were carried out with the CAM-B3LYP/6-31G(d,p) level of theory. The amount of Hartree−Fock exchange in CAM-B3LYP increases from 19% at short-range to 65% at long-range (0.33

Received: July 20, 2014
Revised: September 27, 2014
Published: September 30, 2014

dx.doi.org/10.1021/jp507251e | J. Phys. Chem. A 2014, 118, 10067−10072

range parameter) and should be better than B3LYP at describing the long-range exchange behavior of the density distorted by the strong laser field.[16] The interaction of the molecule with the laser field was calculated in the semiclassical dipole approximation.

$$\hat{\mathbf{H}}(t) = \hat{\mathbf{H}}_{el} - \vec{\mu}\vec{E}(t) \qquad \vec{E}(t) = \vec{s}(t)\sin(\omega t - \phi) \tag{1}$$

$\vec{\mu}$ is the dipole operator, $\vec{E}(t)$ is the electric field component of the laser, and $\vec{s}(t)$ describes the shape of the pulse. The present study used a four-cycle linearly polarized trapezoid pulse

$$\vec{s}(t) = \left(\frac{\omega t}{2\pi}\right)\vec{E}_{max} \qquad \text{for } 0 \le t \le \frac{2\pi}{\omega}$$

$$\vec{s}(t) = \vec{E}_{max} \qquad \text{for } \frac{2\pi}{\omega} \le t \le \frac{6\pi}{\omega}$$

$$\vec{s}(t) = \left(4 - \frac{\omega t}{2\pi}\right)\vec{E}_{max} \qquad \text{for } \frac{6\pi}{\omega} \le t \le \frac{8\pi}{\omega} \tag{2}$$

or a cosine squared pulse

$$\vec{s}(t) = \vec{E}_{max}\cos^2\left(\frac{\omega t}{8} - \frac{\pi}{2}\right) \qquad \text{for } 0 \le t \le \frac{8\pi}{\omega}$$

$$\vec{s}(t) = 0 \qquad \text{otherwise} \tag{3}$$

The 7 μm pulses had maximum field strengths, $\vec{E}_{max}$ of 0.05 and 0.07 au (intensities of 0.88 and 1.7 × 10^{14} W/cm^2, respectively). The direction of the laser field was chosen to be oriented randomly or aligned with the C−X bond axis.

Classical trajectories were integrated using our Hessian-based predictor−corrector algorithm.[17] This method approximates the surface by a distance-weighted interpolant (DWI) using the first and second derivatives of the energy. The first derivative of the gradient with respect to the electric field was also included in the predictor and the corrector steps. The velocity Verlet method with δt = 0.0025 fs was used to integrate both the predictor and corrector steps on the DWI surface. An overall step size of Δt = 0.25 fs was employed, and the Hessian was updated[18,19] for 20 steps before being recalculated analytically. The starting structures had no rotational energy, and zero-point vibrational energy was added to the initial structures using orthant sampling of the momentum.[20] Approximately 100−200 trajectories were calculated for each set of starting conditions. The results of the trajectory calculations are listed in Table S1 of the Supporting Information. A few trajectories dissociated sequentially into multiple fragments; these were classified by the first dissociation event (see Table S1 footnote, Supporting Information). Some of the trajectories showed an unusually high gain in energy. This problem was traced to large charge oscillations when some bonds were stretched to more than 3 Å within the laser pulse. Because the electronic structure was converged at each step of the trajectory integration rather than propagated, the charge on the fragments in some elongated bonds varied from plus to minus as the field changed the sign. These trajectories were discarded as artifacts of the Born−Oppenheimer molecular dynamics approach.

RESULTS AND DISCUSSION

Energetics. The energetics for the fragmentation and isomerization of $CH_3NH_2^+$, CH_3OH^+, and CH_3F^+ were calculated at the CAM-B3LYP/6-31G(d,p) and CBS-QB3 levels of theory and are shown in Figure 1. As in our earlier study of methanol cation,[11] the DFT results agree relatively well with the more accurate calculations. The geometries and more detailed potential energy diagrams can be found in the Supporting Information. In all cases, the lowest-energy channel corresponds to C−H bond cleavage, and the CH_2X^+ product has C−X double bond character (C−N = 1.275, C−O = 1.246, and C−F = 1.233 Å at the CBS-QB3 level of theory). The C−H bond dissociation energies for CH_3OH^+ and CH_3F^+ are ∼9 kcal/mol smaller than those for $CH_3NH_2^+$ at the CBS-QB3 level of theory. A similar trend of closely spaced energies for CH_3OH^+ and CH_3F^+ and higher energies for $CH_3NH_2^+$ is observed for the H_2 elimination reaction and the barrier for 1,2-hydrogen shift isomerization. The isomerization reaction is nearly thermoneutral for $CH_2NH_3^+$ and CH_2FH^+ but slightly exothermic for $CH_2OH_2^+$. The cleavage of the C−X bond can occur before or after isomerization. In both cases, the trend in the dissociation energies is $CH_3NH_2^+$ > CH_3OH^+ > CH_3F^+, which is opposite the ordering for the neutrals (83 kcal/mol for CH_3NH_2, 91 kcal/mol for CH_3OH, and 110 kcal/mol CH_3F at CBS-QB3). This can be understood in terms of orbital interactions. The C−X bonds in the cations dissociate heterolytically, $CH_3X^+ \rightarrow CH_3^+ + X$ and $CH_2XH^+ \rightarrow CH_2^+ + XH$. The C−X bond in the cation is formed by interaction of an X lone pair with an empty carbon p orbital. The lone pair on F is lower in energy than O and interacts more weakly with the empty p on C, resulting in a C−F bond that is weaker than C−O. Similarly, the higher-energy N lone pair interacts more strongly with the carbon p orbital and forms a C−N bond that is stronger than the C−O bond.

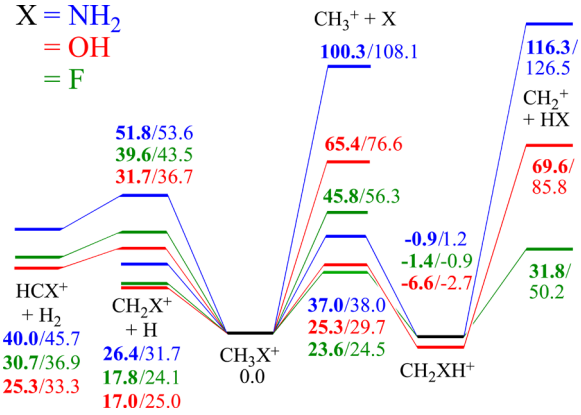

Figure 1. Comparison of the low-energy fragmentation and isomerization channels (in kcal/mol) for $CH_3NH_2^+$ (blue), CH_3OH^+ (red), and CH_3F^+ (green) calculated at the CBS-QB3 (bold) and CAM-B3LYP/6-31G(d,p) levels of theory.

Dynamics. To simulate the isomerization and fragmentation of CH_3X^+ by intense four-cycle 7 μm laser pulses, classical trajectories were calculated on the ground-state potential energy surface of the cation using the CAM-B3LYP/6-31G(d,p) level of theory. Simulations were carried out with trapezoidal-shaped laser pulses to maximize the interaction with the laser. For each field strength, approximately 200 trajectories were calculated for each molecule with the trapezoid pulse. Additional sets of 100 trajectories were computed with cosine squared pulses and a field strength of 0.07 au. Calculations were carried out for molecules oriented randomly in the laser field and for molecules with the C−X bond aligned with the laser polarization. On the basis of work with $ClCHO^+$, CF_3Br^+, and $C_6H_5I^{2+}$,[1,2] alignment of the C−X bond with the laser field should enhance C−X fragmentation and 1,2-hydrogen migration.

dx.doi.org/10.1021/jp507251e | J. Phys. Chem. A 2014, 118, 10067−10072

Table 1. Branching Ratios for the Reactive Trajectories in Percentages for CH_3X^+ (X = NH_2, OH, and F)

molecular species	orientation	field strength and pulse shape	average energy absorbed (kcal/mol)	fraction of trajectories reacting	$CH_2X^+ + H$	$CH_3^+ + X$	CH_2XH^+	$CH_2^+ + HX$	$HCX^+ + H_2$
$CH_3NH_2^+$	random	0.07 au, cosine sq	56.7	0.11	100.0	0.0	0.0	0.0	0.0
		0.05 au, trapezoid	54.1	0.14	92.9	0.0	3.6	0.0	3.6
		0.07 au, trapezoid	112.4	0.56	91.2	1.0	2.0	0.0	5.9[a]
	aligned	0.05 au, trapezoid	112.0	0.59	84.8	1.7	5.9	0.0	7.6
		0.07 au, trapezoid	212.3	0.96	63.0	3.2	0.6	0.0	33.1[b]
CH_3OH^+	random	0.07 au, cosine sq	34.5	0.40	76.9	0.0	0.0	0.0	23.1
		0.05 au, trapezoid	41.8	0.35	82.9	0.0	4.3	0.0	12.9
		0.07 au, trapezoid	80.7	0.73	79.7	0.8	2.5	0.0	16.9[c]
	aligned	0.05 au, trapezoid	75.5	0.72	71.3	0.0	8.4	0.0	20.3
		0.07 au, trapezoid	120.5	0.92	64.6	2.7	4.1	0.0	28.6[d]
CH_3F^+	random	0.07 au, cosine sq	36.3	0.40	82.9	0.0	4.9	4.9	7.3
		0.05 au, trapezoid	33.3	0.34	75.8	1.5	7.6	0.0	15.2
		0.07 au, trapezoid	69.4	0.78	79.6	1.8	2.6	2.6	13.3
	aligned	0.05 au, trapezoid	58.0	0.69	72.5	4.4	7.2	0.7	15.2
		0.07 au, trapezoid	105.0	0.97	67.3	6.7	2.4	6.1	17.6

[a]33.3% of those are $CH_2NH^+ + H_2$. [b]31.4% of those are $CH_2NH^+ + H_2$. [c]30% of these are $CH_2O^+ + H_2$. [d]4.8% of those are $CH_2O^+ + H_2$.

The average amounts of energy gained from the laser pulse are listed in Table 1. A cosine squared pulse with a field strength of 0.07 au deposited approximately the same amount of energy as a trapezoid pulse with a field strength of 0.05 au. This is in accord with the fact that the integrated intensities of these two pulses are nearly equal. For each molecule, the percentage of reactive trajectories correlates very well with the average amount of energy deposited, as shown in Figure 2. In

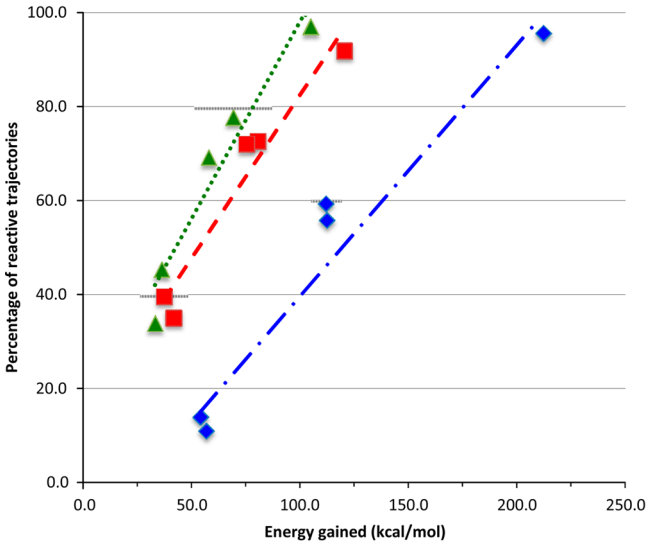

Figure 2. Percentage of reactive trajectories as a function of energy gained (in kcal/mol): (a) $CH_3NH_2^+$ (blue diamonds, dotted−dashed line), (b) CH_3OH^+ (red squares, dashed line), and (c) CH_3F^+ (green triangles, dotted line).

comparing the molecules, it is evident that $CH_3NH_2^+$ requires a larger amount of energy than CH_3OH^+ for the same degree of dissociation. This is in keeping with the larger barriers for $CH_3NH_2^+$. Correspondingly, less energy is needed for CH_3F^+ because it has lower barriers than CH_3OH^+.

The distributions of energy gained by CH_3X^+ (X = NH_2, OH, and F) from the trapezoidal laser pulse are shown in Figure 3. The spread in the energies is over 100 kcal/mol with somewhat longer tails toward higher energies. $CH_3NH_2^+$ gained the most energy from the pulse, and CH_3F^+ gained the least. Increasing the field strength from 0.05 to 0.07 au doubles the intensity (from 0.88 to 1.7 × 10^{14} W/cm^2) and nearly doubles the amount of energy deposited.

Molecules with the C−X axis aligned with the laser polarization gained nearly twice as much energy from the laser pulse as molecules oriented randomly. This can be understood in terms of the vibrational spectra. The difference in intensity of the IR spectra of aligned and rotationally averaged CH_3X^+ are shown in Figure 4 (individual spectra are available in the Supporting Information). When the C−X axis is aligned with the laser polarization, the intensities in the 1000−2000 cm^{-1} range are significantly larger than those for the randomly oriented molecules. The vibrations in this region are primarily C−H bending modes. The distribution of frequencies of a four-cycle 7 μm trapezoidal pulse is centered around 1430 cm^{-1} with a fwhm of ∼600 cm^{-1}. This covers the region where the aligned molecules absorb more strongly than those randomly oriented.

The results of trajectory calculations are summarized in Table 1. As expected from the higher barriers seen in Figure 1, the fraction of trajectories undergoing fragmentation and isomerization reactions for a given pulse shape and intensity is smallest for $CH_3NH_2^+$. Most of the isomerizations and fragmentations occur after the pulse, but the fraction occurring within the pulse grows with increasing energy (reaching 20−25% for CH_3F^+ with a field strength of 0.07 au; see Table S1, Supporting Information). Alignment of the C−X bond with the laser polarization increases the fraction of reactive trajectories as a consequence of the greater amount of energy gained from the pulse.

The branching ratio of various products as percentages for the reactive trajectories are listed in Table 1 and summarized graphically in Figure 5. Of the three low-energy channels, $CH_3X^+ \rightarrow CH_2X^+ + H$ is dominant in all cases, followed by H_2 elimination. Isomerization to CH_2XH^+ is generally the next largest percentage. Although the 0.05 trapezoid pulse and the 0.07 au cosine squared pulse deposit similar amounts of energy, the latter produces less isomerization and $CH_3^+ + X$ dissociation. Compared to randomly oriented molecules, cations with the C−X bond aligned with the laser field have somewhat lower branching ratios for H dissociation and larger

dx.doi.org/10.1021/jp507251e | J. Phys. Chem. A 2014, 118, 10067−10072

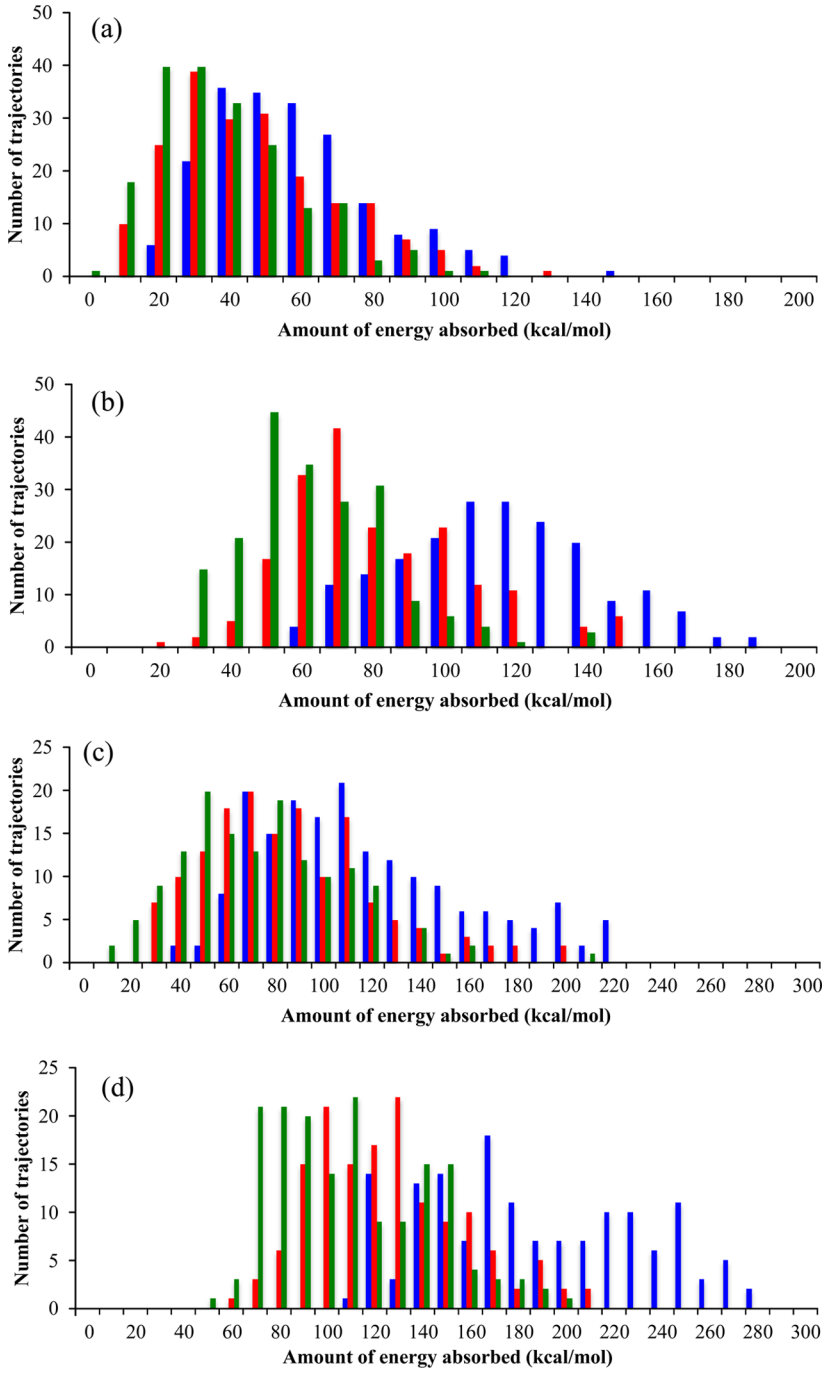

Figure 3. Histograms of the distribution of vibrational energy absorbed by CH_3X^+ (X = NH_2 (blue), OH (red), and F (green)) from a 95 fs, 7 μm trapezoidal laser pulse as a function of molecular orientation and maximum field strength: (a) random orientation, 0.05 au field, (b) C−X aligned, 0.05 au field, (c) random orientation, 0.07 au field, and (d) C−X aligned, 0.07 au field.

branching ratios for the other channels. Although the number of trajectories is small, alignment results in a factor of 3 increase in CH_3^+ + X dissociation for several cases. For isomerization of CH_3OH^+ to $CH_2OH_2^+$, the increase is nearly a factor of 2.

For $CH_3NH_2^+$, little or no C−N bond breaking is seen, in keeping with the high dissociation energy. Only when the molecule is aligned with the field is a small amount of CH_3^+ + NH_2 obtained. Isomerization and H_2 elimination are roughly comparable in magnitude. Even though the latter has a higher barrier, it is a looser transition state. The large percentage of H_2 elimination for aligned $CH_3NH_2^+$ with 7 μm and a 0.07 field strength can be attributed to the large amount of energy gained from the pulse (212 kcal/mol).

The results for CH_3OH^+ in 800 nm and 7 μm laser fields have been reported previously.[11,12] Compared to $CH_3NH_2^+$, CH_3OH^+ in a 7 μm laser field produces significantly more H_2 elimination than isomerization. This is in accord with the smaller difference in the two barrier heights in CH_3OH^+ compared to that in $CH_3NH_2^+$. Alignment of the C−O bond with the laser field enhances the $HCOH^+$ + H_2 and $CH_2OH_2^+$ channels when compared to random orientation with the same laser parameters.

dx.doi.org/10.1021/jp507251e | J. Phys. Chem. A 2014, 118, 10067−10072

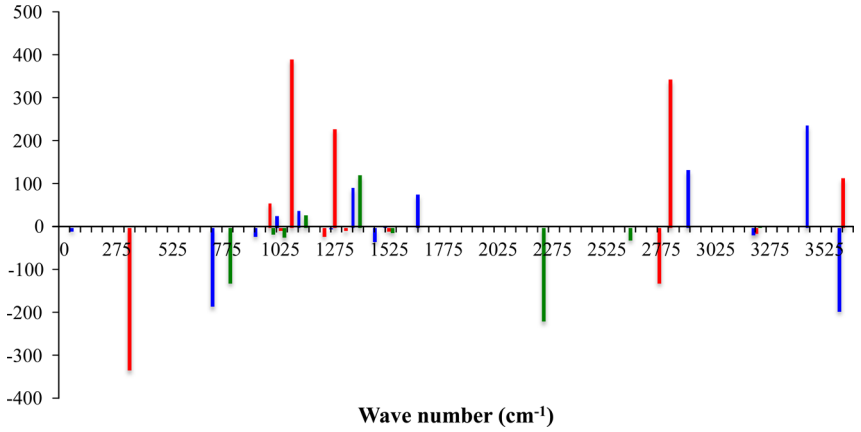

Figure 4. Difference in IR intensities (aligned, random) for $CH_3NH_2^+$ (blue), CH_3OH^+ (red), and CH_3F^+ (green).

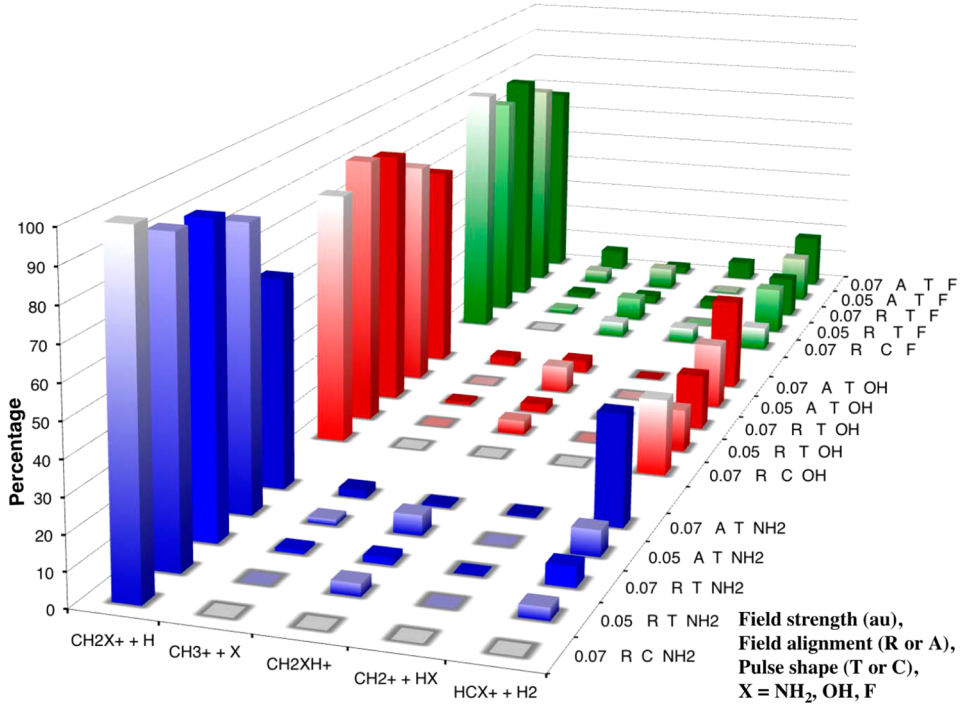

Figure 5. Branching ratios for $CH_3NH_2^+$ (blue), CH_3OH^+ (red), and CH_3F^+ (green) for cosine squared (C) and trapezoid (T) pulse shapes with field strengths of 0.5 and 0.7 au and randomly oriented (R) or aligned (A) with the C−X bond.

Of the three molecules, CH_3F^+ shows the most C−X dissociation, as expected from the fact that it has the lowest C−X bond dissociation energies. Only CH_3F^+ shows a significant amount of C−X dissociation after isomerization, and this is highest when the C−F bond is aligned with the field. However, alignment has little effect on isomerization.

SUMMARY

Energetics of the methylamine, methanol, and methyl fluoride cations were studied at the CAM-B3LYP/6-31G(d,p) and CBS-QB3 levels of theory. For all three molecules studied, isomerization, H elimination, and H_2 elimination were found to be low-energy reaction pathways.

The isomerization reaction was nearly thermoneutral for $CH_2NH_3^+$ and CH_2FH^+ but slightly exothermic for $CH_2OH_2^+$. Ab initio classical trajectory calculations were carried out with the CAM-B3LYP/6-31G(d,p) level of theory on the ground-state potential energy surface in the presence of a four-cycle, 95 fs, 7 μm laser pulse with maximum field strengths of 0.05 and 0.07 au (equivalently, intensities of 0.88 and 1.7 × 10^{14} W/cm^2). The amount of energy absorbed was nearly doubled when the laser field was aligned along the C−X axis and also when the field strength was increased from 0.05 to 0.07 au. The most abundant reaction path was CH_2X^+ + H (63%−100%), with HCX^+ + H_2 (0−33%) the second most abundant. Out of all of the trajectories studied, dissociation after isomerization was observed only in CH_3F^+ (0−6%). Alignment of the C−X bond with the laser field increased the amount of CH_3^+ + X dissociation for all three molecules. Alignment also increased the branching ratio for isomerization in CH_3OH^+ and H_2 elimination in $CH_3NH_2^+$ and CH_3OH^+.

ASSOCIATED CONTENT

Supporting Information

Detailed potential energy diagrams for methylamine, methanol, and methyl fluoride cations, a summary of trajectory data,

dx.doi.org/10.1021/jp507251e | J. Phys. Chem. A 2014, 118, 10067−10072

individual IR spectra for the three monocations aligned with the laser field and rotationally averaged, and structures and Cartesian coordinates for selected molecules. This material is available free of charge via the Internet at http://pubs.acs.org.

AUTHOR INFORMATION

Corresponding Author

*E-mail: hbs@chem.wayne.edu. Phone: 1-313-577-2562. Fax: 1-313-577-8822.

Notes

The authors declare no competing financial interest.

ACKNOWLEDGMENTS

This work was supported by a grant from the National Science Foundation (CHE1212281). Wayne State University's computing grid provided computational support.

REFERENCES

(1) Lee, S. K.; Suits, A. G.; Schlegel, H. B.; Li, W. A Reaction Accelerator: Mid-Infrared Strong Field Dissociation Yields Mode-Selective Chemistry. *J. Phys. Chem. Lett.* **2012**, *3*, 2541−2547.

(2) Lee, S. K.; Schlegel, H. B.; Li, W. Bond-Selective Dissociation of Polyatomic Cations in Mid-Infrared Strong Fields. *J. Phys. Chem. A* **2013**, *117*, 11202−11209.

(3) Furukawa, Y.; Hoshina, K.; Yamanouchi, K.; Nakano, H. Ejection of Triatomic Hydrogen Molecular Ion from Methanol in Intense Laser Fields. *Chem. Phys. Lett.* **2005**, *414*, 117−121.

(4) Okino, T.; Furukawa, Y.; Liu, P.; Ichikawa, T.; Itakura, R.; Hoshina, K.; Yamanouchi, K.; Nakano, H. Coincidence Momentum Imaging of Ejection of Hydrogen Molecular Ions from Methanol in Intense Laser Fields. *Chem. Phys. Lett.* **2006**, *419*, 223−227.

(5) Okino, T.; Furukawa, Y.; Liu, P.; Ichikawa, T.; Itakura, R.; Hoshina, K.; Yamanouchi, K.; Nakano, H. Ejection Dynamics of Hydrogen Molecular Ions from Methanol in Intense Laser Fields. *J. Phys. B* **2006**, *39*, S515−S521.

(6) Liu, P.; Okino, T.; Furukawa, Y.; Ichikawa, T.; Itakura, R.; Hoshina, K.; Yamanouchi, K.; Nakano, H. Three-Body Sequential Coulomb Explosions of CH_3OD^{3+} Induced by Intense Laser Fields. *Chem. Phys. Lett.* **2006**, *423*, 187−191.

(7) Okino, T.; Furukawa, Y.; Liu, P.; Ichikawa, T.; Itakura, R.; Hoshina, K.; Yamanouchi, K.; Nakano, H. Coincidence Momentum Imaging of Ultrafast Hydrogen Migration in Methanol and Its Isotopomers in Intense Laser Fields. *Chem. Phys. Lett.* **2006**, *423*, 220−224.

(8) Itakura, R.; Liu, P.; Furukawa, Y.; Okino, T.; Yamanouchi, K.; Nakano, H. Two-Body Coulomb Explosion and Hydrogen Migration in Methanol Induced by Intense 7 and 21 fs Laser Pulses. *J. Chem. Phys.* **2007**, *127*, 104306.

(9) Xu, H.; Marceau, C.; Nakai, K.; Okino, T.; Chin, S.-L.; Yamanouchi, K. Communication: Two Stages of Ultrafast Hydrogen Migration in Methanol Driven by Intense Laser Fields. *J. Chem. Phys.* **2010**, *133*, 071103.

(10) Xu, H.; Okino, T.; Kudou, T.; Yamanouchi, K.; Roither, S.; Kitzer, M.; Batuska, A.; Chin, S.-L. Effect of Laser Parameters on Ultrafast Hydrogen Migration in Methanol Studied by Coincidence Momentum Imaging. *J. Phys. Chem. A* **2012**, *116*, 2686−2690.

(11) Thapa, B.; Schlegel, H. B. Molecular Dynamics of Methanol Monocation (CH_3OH^+) in Strong Laser Fields. *J. Phys. Chem. A* **2014**, *118*, 1769−1776.

(12) Thapa, B.; Schlegel, H. B. Molecular Dynamics of Methanol Monocation (CH_3OH^+) in Strong Laser Fields: Comparison of 800 nm and 7 micron Laser Fields. *Chem. Phys. Lett.* **2014**, *610*−*611*, 219−222.

(13) Frisch, M. J.; Trucks, G. W.; Schlegel, H. B.; Scuseria, G. E.; Robb, M. A.; et al. *Gaussian Development Version*, revision H.35; Gaussian, Inc.: Wallingford, CT, 2014.

(14) Montgomery, J. A.; Frisch, M. J.; Ochterski, J. W.; Petersson, G. A. A Complete Basis Set Model Chemistry. VI. Use of Density Functional Geometries and Frequencies. *J. Chem. Phys.* **1999**, *110*, 2822−2827.

(15) Yanai, T.; Tew, D. P.; Handy, N. C. A New Hybrid Exchange−Correlation Functional Using the Coulomb-Attenuating Method (CAM-B3LYP). *Chem. Phys. Lett.* **2004**, *393*, 51−57.

(16) Sonk, J. A.; Schlegel, H. B. TD-CI Simulation of the Electronic Optical Response of Molecules in Intense Fields II: Comparison of DFT Functionals and EOM-CCSD. *J. Phys. Chem. A* **2011**, *115*, 11832−11840.

(17) Schlegel, H. B. Molecular Dynamics in Strong Laser Fields: A New Algorithm for Ab Initio Classical Trajectories. *J. Chem. Theory Comput.* **2013**, *9*, 3293−3298.

(18) Bakken, V.; Millam, J. M.; Schlegel, H. B. Ab Initio Classical Trajectories on the Born− Oppenheimer Surface: Updating Methods for Hessian-Based Integrators. *J. Chem. Phys.* **1999**, *111*, 8773−8777.

(19) Wu, H.; Rahman, M.; Wang, J.; Louderaj, U.; Hase, W. L.; Zhuang, Y. Higher-Accuracy Schemes for Approximating the Hessian from Electronic Structure Calculations in Chemical Dynamics Simulations. *J. Chem. Phys.* **2010**, *133*, 074101.

(20) Bunker, D. L.; Hase, W. L. Non-RRKM Unimolecular Kinetics — Molecules in General, and CH_3NC in Particular. *J. Chem. Phys.* **1973**, *59*, 4621−4632.